

Photoemission study of Al adlayers on MnR. S. Dhaka,^{1,*} A. K. Shukla,^{1,†} K. Horn,² and S. R. Barman¹¹*Surface Physics Laboratory, UGC-DAE Consortium for Scientific Research, Khandwa Road, Indore, 452001 Madhya Pradesh, India*²*Fritz-Haber-Institut der Max-Planck-Gesellschaft, Faradayweg 4-6, DE-14195 Berlin, Germany*

(Received 5 August 2011; revised manuscript received 15 November 2011; published 7 December 2011)

Al overlayers on Mn, studied by photoemission spectroscopy, show a large lowering of the Al $2p$ core-level binding energy by 0.5 eV at submonolayer (0.1 ML) coverage. The binding energy increases with coverage and reaches the bulk Al value at ≈ 1.3 ML. The Al $2p$ core-level spectrum exhibits extra components related to the different chemical environment at the interface, which decrease in intensity with increasing Al coverage. The Al related plasmon loss features appear above 1 ML. The present results are explained by a strong Al s , p -Mn $3d$ hybridization at the submonolayer coverage due to interface alloying, whose influence on the spectra is dominated by metallic bonding in the Al layer as coverage increases. The valence-band spectra demonstrate systematic suppression of Mn $3d$ -like states and emergence of a parabolic free-electron-like Al density of states.

DOI: [10.1103/PhysRevB.84.245404](https://doi.org/10.1103/PhysRevB.84.245404)

PACS number(s): 79.60.Dp, 73.20.Mf, 73.21.—b

I. INTRODUCTION

The properties of heteroepitaxial growth of adlayers are currently a topic of broad interest, motivated by technological applications such as magnetic data storage and nanoelectronic devices. To fabricate these devices, one requires the control of the growth modes adopted by thin films deposited on a substrate.^{1–11} It is quite remarkable that the substrate plays an important role in the electronic properties of metallic adlayers where the interactions with the substrate material are crucial.^{1–5} This can provide valuable information about the growth modes of thin films and intermixing phenomena at the interfaces. The core-level binding energy (BE) shift and line-shape change with increasing film coverage, which allows for a deeper understanding of the physical mechanism underlying final-state effects where changes occur in the screening of the core hole due to the different chemical environment of the adatoms. In general, the properties of low dimensional systems, e.g., ultrathin films and surface alloys, can be quite different from their bulk properties.^{6–11} It was shown that the metals deposited on substrate can occupy the topmost surface sites, diffuse into the subsurface, and alloy formation occurs at the intermixed regime of bimetallic surfaces.¹² The migration of Al atoms and formation of complex surface alloy phases were observed by using scanning tunneling microscopy (STM).^{6,7} Al is a nearly free-electron metal, and in the bulk Al-Mn alloys the Mn magnetic moment has been reported to depend on the extent of Mn $3d$ -Al $3s$, p hybridization.¹³ It is found that Mn grows in a layer-by-layer fashion on the Al(111) surface, and the changes in BE and line shape have been reported for different coverages.¹⁴ Al overlayers on Mn are of particular interest, since in bulk Al-Mn alloys the s , p - d hybridization is of great significance in determining the electronic structure and can even give rise to a pseudogap at the Fermi level.¹⁵ Therefore, the general goal of the present work is to see how the electronic structure of Al changes as one goes from the submonolayer to the monolayer of coverages on the Mn substrate.

Al adlayers have been studied on different metal substrates: For example, Di Marzio *et al.* studied the growth and modifications of Al on Ta(110) as a function of Al coverage and temperature by using photoemission spectroscopy.¹ They

found no intermixing at room temperature and an Al $2p$ core-level shift toward higher BE with increasing Al coverage. An electronic state was observed in the valence band, which was related to the hybridization between Ta $5d$ and Al $3s$, p states. A layer-by-layer growth of Al on Pt(111) has been found at 160 K without any significant intermixing.³ However, at 300 K, after completion of the first monolayer, Al-Pt surface alloying has been reported. Layer-by-layer growth of Al on Mo(110) was reported by Kdaczkiwicz *et al.*⁴ Andersen *et al.* observed the BE shift in the Al $2p$ core level as a function of Al coverage on Mo(110), and these results have been explained in terms of adhesion and interface segregation energies.⁵ Low-energy electron diffraction (LEED) has been used to investigate the growth mode of Al on Ta(110), and five different phases of Al have been observed for different substrate temperatures.¹⁶ At room temperature, Pd intermixing with Al and surface alloy formation have been related to the interaction between Pd and Al through the hybridization of the Pd d and Al s states.^{17–19}

The present study is motivated by our earlier work on Mn adlayers on the Al(111) surface,^{14,15,20} where interesting changes in both Mn $2p$ and Al $2p$ core-level line shapes were observed.¹⁴ In particular, a satellite peak in the Mn $2p_{3/2}$ spectrum of bulklike Mn layers has been observed at a 1 eV higher BE by high-resolution photoemission study.²⁰ The origin of this satellite feature is due to an intra-atomic multiplet effect related to Mn atoms with large local moment. Interestingly, in a reverse experiment where Al was deposited on the thick Mn layer, the intensity of the 1 eV satellite in the Mn $2p_{3/2}$ core-level spectrum was found to decrease with increasing Al coverage [see Fig. 3(b) of Ref. 20]. The suppression of the 1 eV satellite feature was explained by the enhanced hybridization between Mn $3d$ and Al s , p states.^{15,20,21} For Mn/Al(111), it has been found that an extra feature emerges in the Al $2p$ core-level spectrum toward lower BE with increasing Mn coverage.¹⁴ The authors suggested that the origin of this extra feature is related to interface alloying. The shift of the interface alloying related component in the Al $2p$ spectra toward lower BE with increasing Mn coverage indicates changes in final-state screening or initial-state related charge redistribution due to alloying.¹⁴ However, this feature

was not clearly resolved due to the limited energy resolution of the x-ray photoemission experiments.¹⁴ Therefore, the need for doing these experiments using synchrotron radiation with high resolution and intensity was realized. Although some earlier studies have been reported on Al adlayers deposited on different substrates, no work exists in the literature on Al submonolayers on Mn. In this paper, we present high-resolution Al $2p$ core-level spectra and valence bands of Al overlayers on Mn grown at room temperature.

II. EXPERIMENTAL

The experiments were performed by using an EA 125 commercial electron energy analyzer from Omicron GmbH, Germany, at a base pressure of 5×10^{-11} mbar in the experimental chamber. These measurements were done on the undulator-based UE 56/2-PGM 1 beamline,²² at Berliner Elektronenspeicherring-Gesellschaft für Synchrotronstrahlung in Berlin, Germany. An electropolished Al(111) single crystal was cleaned by repeated cycles of sputtering using 1-2 keV Ne^+ and subsequent annealing at 723 K to regenerate surface order.²³ A thick layer of Mn, which acted as a template for the Al adlayers, was prepared by depositing high-purity Mn on an Al(111) substrate using a water cooled Knudsen cell.²⁴ During the deposition, the substrate, mounted on a specially designed sample holder,²⁵ was held at room temperature and a thick Mn layer was deposited that was not crystalline, as shown in our earlier work.¹⁴ High-purity (99.999%) aluminum layers were prepared on the thick layer of Mn at the rates of 0.04–0.06 Å/min. During the metal evaporation, the chamber pressure was kept below 3.5×10^{-10} mbar. One monolayer (ML) is defined to be a close packed Al layer with a thickness of 2.5 Å.²⁶ After each deposition, O 1s and C 1s signals were recorded to ensure the absence of oxygen and carbon contamination. The overall energy resolution was estimated to be about 140 and 170 meV at 105 and 200 eV photon energies, respectively. The Al $2p$ spectra were fitted by using a Doniach-Šunjić (DS) line-shape²⁷ convoluted with experimental broadening parameters. The intrinsic lifetime broadenings of the core level (2γ), the DS asymmetry parameter (α), intensities, peak positions, and the iterative background parameter are varied independently during fitting, as in our previous work.²⁸ During the fitting of the Al $2p$ core-level spectra, we notice a hump at about the 73.7 eV BE where an additional small Gaussian peak (not shown) has been used to simulate the spectra. Since Mn is highly reactive, this is possibly due to slight oxygen contamination on the Mn substrate, which is estimated to be less than 2%.

III. RESULTS AND DISCUSSION

The Al $2p$ core-level spectra as a function of Al coverage on a thick layer of Mn are compared with the Al $2p$ core level from clean Al(111) (top spectrum) in Fig. 1. At ultralow coverage (0.1 ML), the Al $2p_{3/2}$ peak appears at about 72.3 eV and, clearly, the BE increases with coverage. For highest Al coverage (1.3 ML), the Al $2p_{3/2}$ BE is 72.8 eV, which is close to the BE of Al(111). Thus, a large shift of 0.5 eV in the Al $2p$ peak is observed between 0.1 and 1.3 ML. The line shapes also

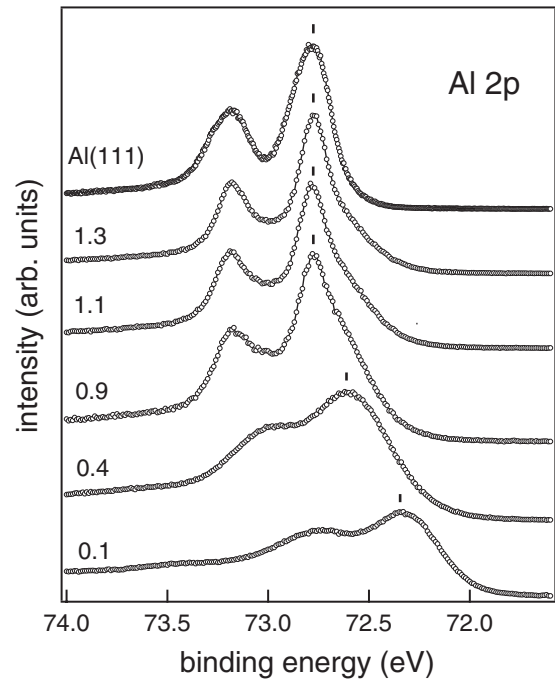


FIG. 1. Al $2p$ core-level spectra as a function of Al coverage on Mn measured with 200 eV photon energy. The spectra have been shifted along the vertical axis for clarity of presentation. The coverage (ML) is indicated for each spectrum.

change considerably with coverage. At the lowest coverage, a large asymmetry toward lower BE is observed, which becomes more symmetric at higher coverage. Similar changes in BE and line shape for the Al $2p$ core level have also been observed for the spectra recorded with 105 eV photon energy. The observed large asymmetry suggests the presence of extra features in the Al $2p$ spectra.

To understand the change in BE and line shape, the Al $2p$ core-level spectra for different Al coverages have been fitted and compared with that of clean Al(111) (Fig. 2). In order to get a satisfactory least-squares fit, the spectra were fitted with three components (Figs. 2 and 3), marked by A_1 , A_2 , and A_3 , where each component has spin-orbit splitting peaks ($2p_{3/2}$ and $2p_{1/2}$). The branching ratio of the spin-orbit split peaks are kept fixed for the three components for all coverages. A fitting with two components allowing for variation in lifetime and Gaussian broadenings did not produce satisfactory fits. In the case of 0.4 ML, the spectrum could not be fitted using the instrumental broadening parameters, and it was obvious that there is an extra broadening. Hence, an extra Gaussian broadening was used for the 0.4 ML spectrum. This extra broadening is possibly due to the random distribution of the Al atoms at inequivalent sites on the Mn substrate.

It is clear from Figs. 2(a)–2(d) that, for 0.4 ML, A_2 and A_3 are dominant (A_3 being about half of A_2) and there is hardly any contribution from A_1 . However, at 0.9 ML, the A_1 component increases drastically and dominates over the other two. At higher coverages (1.1–1.3 ML), A_2 and A_3 decrease further. The values of the parameters such as BE, α , and γ are 72.78 eV ($2p_{3/2}$), 0.11, and 30 meV, respectively, for the A_1 component for 1.3 ML. These values are quite similar to that of clean Al(111) crystal (BE, α , and γ are 72.8 eV ($2p_{3/2}$),

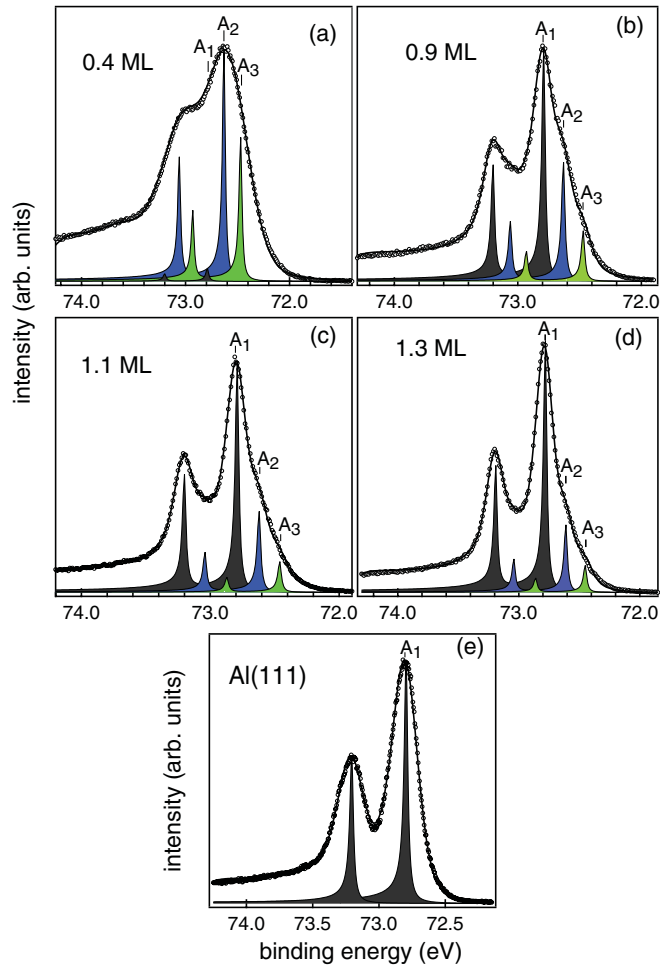


FIG. 2. (Color online) Al $2p$ core-level spectra (open circles) recorded with 200 eV photon energy, the fitted spectra (thick solid line), and the DS line-shape components (shaded) obtained from least-squares fitting, for (a–d) different Al coverages on Mn, as indicated, and (e) clean Al(111) surface. Different Al $2p$ fitting components are marked by A_1 (dark gray), A_2 (blue), and A_3 (green). The extra Gaussian broadening given to the components in (a) is not shown.

0.1, and 30 meV, respectively).²⁹ Thus, it is clear that the A_1 component corresponds to pure Al [Fig. 2(e)].

Note that, in contrast to Ref. 14, by selecting the appropriate photon energy in this study, we are particularly sensitive to the surface region. For example, the inelastic mean free path (IMFP) of the Al $2p$ photoelectrons is most surface sensitive³⁰ (≈ 4.5 Å) for 105 eV photon energy, while it is ≈ 20 Å for the Mg K_{α} ($h\nu = 1253.6$ eV) source used in Ref. 14. Therefore, to find how the relative intensities of these extra components vary with photon energy, we have also fitted the Al $2p$ core levels measured with 105 eV photon energy (Fig. 3). Our detailed analysis (Figs. 2 and 3) reveals that the large BE shift of Al $2p$ with coverage is related to the change in relative intensities of the components, A_2 and A_3 . These are dominant at submonolayer coverages which appear at about a 0.2 and 0.5 eV lower BE, respectively, compared to A_1 . As coverage increases, A_1 dominates, leading to the overall BE shift. In Fig. 4, we have plotted the relative intensity variations of A_1 , A_2 , and A_3 that were determined by dividing the area under

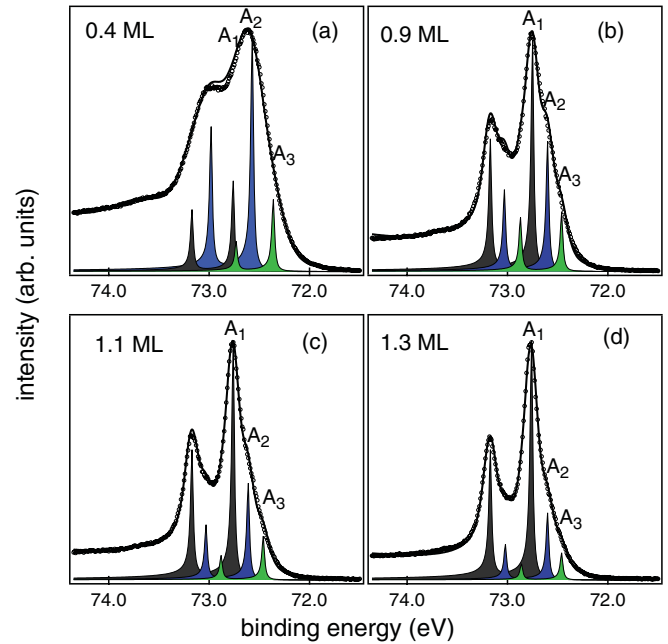


FIG. 3. (Color online) Al $2p$ core-level spectra (open circles) recorded with 105 eV photon energy and the fitted spectra (thick solid line). The DS line-shape components (shaded) obtained from least-squares fitting are shown similar to Fig. 2.

each peak by the total area. This way we can directly compare the relative intensity of each component. Figure 4 clearly shows that the contribution in the total intensity is dominated from the intermixed region (discussed later) at submonolayer coverages (A_2 , A_3 components). However, at higher coverages, the main contribution is from the pure Al related peak (A_1).

We explain the intensity variation of the components in the Al $2p$ peak and the resulting BE shift in the following possible ways. At low coverages (≤ 0.4 ML), only a few Al adatoms are deposited on Mn. In this case, Al adatoms are surrounded mainly by Mn atoms. These Al atoms would participate mainly in Mn d -Al s , p bonding, which significantly lowers the Al $2p$ BE and introduces an extra broadening in the Al $2p$ spectrum toward the lower BE side. A signature of extra broadening in the Al $2p$ core-level spectra was observed with Mn adlayers on the Al(111) surface studied with a Mg K_{α} source.¹⁴ However,

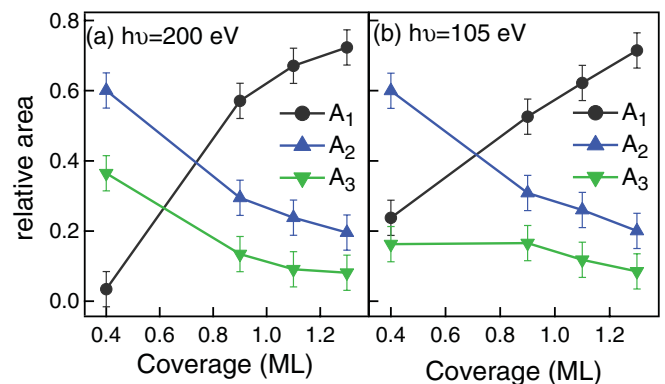


FIG. 4. (Color online) Relative area of peaks A_1 (dark gray), A_2 (blue), and A_3 (green) as a function of Al coverage measured with (a) 200 eV and (b) 105 eV photon energies.

in the present case, we are particularly sensitive (discussed above) to the interface region and therefore observe extra components toward lower BE instead of only a broadening in the spectra. Note that an interesting study by Buchanan *et al.* showed that the intermixing lengths for Al on transition metals (TM) are considerably smaller than those for TM on Al.³¹ Relating to the present study, another possibility might be that the Al atoms diffuse into the Mn substrate and form the intermixed region, i.e., interface alloying of a certain length where Al adatoms experience strong screening and hybridization effects.^{14,15,31} This indicates that these extra components (A_2 and A_3 in the submonolayer coverage) in the Al $2p$ spectra are originating from Al atoms present in the intermixed region. The core hole created in this region during the photoemission process are over screened by the substrate related Mn atoms. The decrease in intensity of these extra components (A_2 and A_3) in the Al $2p$ spectra with increasing Al coverage indicates that the alloy formation is restricted only on the interface region, since at higher coverage the incoming Al adatoms start forming the pure Al layer. Another possible reason for the occurrence of two extra components in the submonolayer region could be related to the different sites available for Al adsorption on Mn. The A_3 component could occupy a hollow position with a higher Mn d -Al s, p overlap, while the A_2 component may result from Al atoms adsorbed at on-top sites. This is consistent with the observed lower BE of the A_3 component than A_2 , where the photoemission signal from the strongly intermixed subsurface region contributes in A_3 and that from the weakly intermixed surface region contributes in A_2 . However, a detailed study of the interface structure with LEED and STM is required to resolve this issue.

We now discuss the intensity variation of the A_1 component (Fig. 4). Note that there is also a finite probability for the existence of pure Al adatoms on the top of the intermixed layer. The photoemission signal from these Al atoms contributes to A_1 . Therefore, in the submonolayer coverage, A_1 has the lowest intensity and the highest BE due to very few unmixed Al atoms and a poorly screened final state, respectively. However, with increase in the Al coverage beyond 1 ML, the s, p hybridization between the Al atoms increases as the number of Al adatoms increases (adatom-adatom interaction dominates), and consequently the BE changes. An increasing Al coverage results in a higher intensity of A_1 and consequently a lower intensity of A_2 and A_3 due to the finite mean-free-path effect and an ensuing lower signal from the buried interface. Above ≈ 1.0 ML, there is hardly any shift or change in line shape in the Al $2p$ core level. Thus, these results show that the nature of surface intermixing and hybridization changes, in particular, in the submonolayer regime. If we compare the relative intensities of different peak components (A_1 , A_2 , and A_3) measured with 200 and 105 eV photon energies (Fig. 4), then we find that the trends are similar. However, for 0.4 ML, there is small quantitative difference in A_1 and A_3 . This small difference might be due to small change in the IMFP of Al $2p$ photoelectrons, between 200 and 105 eV photon energies, which is calculated to be ≈ 5.75 and ≈ 4.5 Å, respectively.³⁰ This indicates a slight increase in the surface sensitivity at 105 eV, which can be effective at submonolayer coverage (0.4 ML) and may result in the contributions mainly from A_1 (pure Al residing at the top surface) and A_2 (weakly intermixed

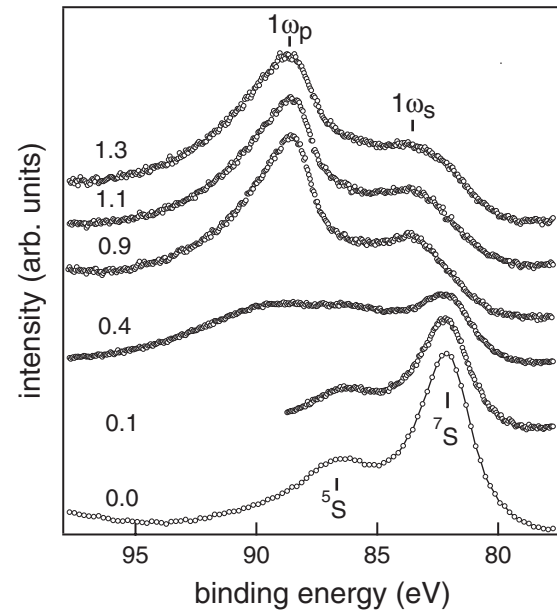


FIG. 5. Mn $3s$ spectra along with the Al related bulk ($1\omega_p$) and surface ($1\omega_s$) plasmon features as a function of Al thickness on Mn. The spectra have been recorded with $h\nu = 350$ eV. The coverage (ML) is shown for each spectrum.

surface region) components, while, for 200 eV, the contributing signal may dominate from the A_2 and A_3 (strongly intermixed subsurface region) components. This is also in agreement with our explanation, discussed above, that the contribution in A_2 and A_3 could be from two different intermixed regions, i.e., the surface and subsurface, respectively.

The substrate related Mn $2p$ core levels (not shown here) show no discernible change in BE as a function of Al coverage. This indicates that there is hardly any charge transfer between Al and Mn atoms. This is consistent with our previous study on Mn adlayers on Al(111), where no charge-transfer-related BE shift was observed in the core-level spectra.^{14,20}

After studying the core-level spectra, we now turn to the measurements where the evolution of the plasmon features in the Al $2p$ core levels can be observed. However, the appearance of the Mn $3s$ core level in the plasmon energy region makes it difficult to study the Al plasmons. To overcome this difficulty, we chose a photon energy of 350 eV, where the Mn $3s$ intensity is less due to a lower photoionization cross section.³² Figure 5 shows the Al $2p$ related plasmons loss features (bulk plasmon, $1\omega_p$ and surface plasmon, $1\omega_s$). For the Mn substrate (0 ML), the Mn $3s$ level shows clear exchange splitting (i.e., the separation between the $7S$ and $5S$ peaks) of about 4.4 eV (Fig. 5). At 0.4 ML Al coverage, a significant decrease in the Mn $3s$ core level has been observed and the Al related plasmons start appearing. Around 1 ML, the Al bulk and surface plasmons are clearly evident at about 88.7 and 83.6 eV Bes (Fig. 5), i.e., 16 and 10.4 eV loss energies, respectively, which are very close to the reported loss features for the clean Al surface.^{33,34} The appearance of plasmons above ≈ 1.0 ML further supports the above proposition of enhanced Al s, p -Al s, p interaction that explains the Al $2p$ BE shift in the submonolayer region where the Mn $3d$ -Al s, p interaction is more predominant. To be noted here is that alkali-metal core-level spectra also show

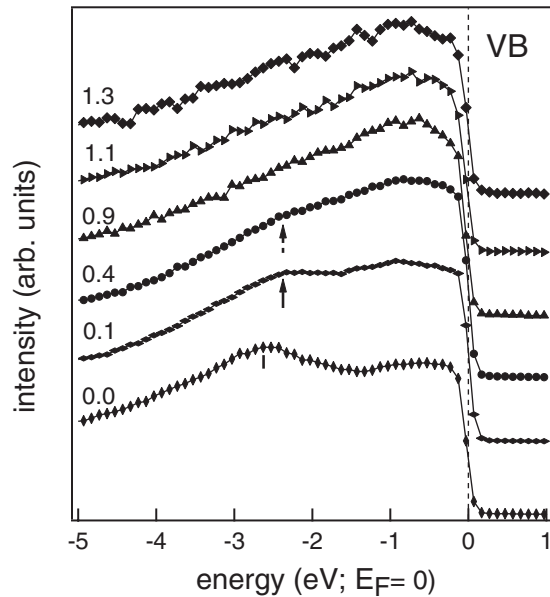


FIG. 6. Valence-band photoemission spectra of Al adlayers on Mn as a function of Al coverage recorded with 200 eV photon energy.

the appearance of a plasmon feature at ≈ 1.0 ML saturation coverage, where a layer-by-layer growth was reported and no charge transfer with the substrate was observed.³⁵

The changes in the valence-band spectra as a function of Al coverage are shown in Fig. 6. The bottom spectrum has been measured for clean Mn (0 ML). It shows a broad feature (marked by a tick) at about the 2.6 eV BE, which represents the Mn $3d$ states. Hobbs *et al.* have calculated the density of states (DOS) of α -Mn using *ab initio* spin-density functional formalism.³⁶ The DOS exhibits the most intense peak around the 2.65 eV BE dominated by Mn $3d$ -like states, which is in excellent agreement with the measured valence band for a clean thick Mn layer (Fig. 6). The Mn valence band also agrees with the experimentally reported ultraviolet photoemission spectra for Mn metal.^{37,38} The valence-band (VB) spectral shape changes even for 0.1 ML Al coverage, and a significant

decrease in the intensity of Mn $3d$ states occurs with a shift of ≈ 0.3 eV (shown by a solid arrow) toward lower BE, which is the signature of the strong Al s , p -Mn $3d$ hybridization. At 0.4 ML, the peak intensity decreases further (shown by a dashed arrow), and, as the coverage is increased, the shape of the valence band tends to the characteristic parabolic shape of Al metal at about 1.0 ML. The significant modification in the valence-band spectra, even in the submonolayer region, and the absence of Mn related features at about 1.0 ML Al coverage suggest that the substrate Mn layer is smooth and the first Al layer grows uniformly. In our earlier work, a layer-by-layer growth mode has been reported for Mn deposition on the Al(111) surface.¹⁴

IV. CONCLUSION

Our photoemission study of Al adlayers on Mn shows that the Al $2p$ core level exhibits a shift of 0.5 eV toward a higher binding energy with increasing coverage, and, at about 1.3 ML, the binding energy is similar to bulk Al. Interesting changes in line shape and extra components in the Al $2p$ core-level spectra have been observed between submonolayer and monolayer coverages. These changes are related to the modification of the bonding characteristics, for submonolayer coverages where Al s , p -Mn $3d$ hybridization dominates due to interface alloying, while, above 1.0 ML, Al s , p -Al s , p interaction dominates. This is also supported by the appearance of Al related plasmons above 1.0 ML coverage. The valence-band spectra exhibit systematic suppression of Mn $3d$ -like states and the emergence of parabolic free-electron-like Al density of states with increasing coverage.

ACKNOWLEDGMENTS

We thank W. Mahler and B. Zada for providing technical help in operating the beamline and the Berliner Elektronenspeicherring-Gesellschaft für Synchrotronstrahlung staff for support. D. P. Woodruff and D. I. Sayago are thanked for useful discussions. Funding from the Max Planck Partner Group Project is gratefully acknowledged.

*Present address: Division of Materials Science and Engineering, The Ames Laboratory, US Department of Energy and Department of Physics and Astronomy, Iowa State University, Ames, IA 50011, USA; rsdhaka@ameslab.gov.

†Present address: National Physical Laboratory, Dr. K. S. Krishnan Marg, New Delhi 110012, India.

¹D. Di Marzio, M. W. Ruckman, S. L. Qiu, L. Jiang, J. Chen, and M. Strongin, *Phys. Rev. B* **39**, 5591 (1989).

²R. Sporken, P. A. Thiry, E. Petit, J. J. Pireaux, R. Caudano, J. Ghijsen, R. L. Johnson, and L. Ley, *Phys. Rev. B* **35**, 7927 (1987).

³K. Wilson, J. Brake, A. F. Lee, and R. M. Lambert, *Surf. Sci.* **387**, 257 (1997).

⁴J. Kdaczkiwicz, M. Hoch, and S. Zuber, *Surf. Sci.* **247**, 284 (1991).

⁵J. N. Andersen, O. Bjorneholm, A. Stenborg, A. Nilsson, C. Wigren, and N. Martensson, *J. Phys. Condens. Matter* **1**, 7309 (1989).

⁶B. Fischer, H. Brune, J. V. Barth, A. Fricke, and K. Kern, *Phys. Rev. Lett.* **82**, 1732 (1999).

⁷T. Duguet, E. Gaudry, T. Deniozou, J. Ledieu, M. C. de Weerd, T. Belmonte, J. M. Dubois, and V. Fournée, *Phys. Rev. B* **80**, 205412 (2009).

⁸G. Bozzolo, J. E. Garcé, and R. J. Smith, *Surf. Sci.* **583**, 229 (2005).

⁹W. J. Wytenburg, R. M. Ormerod, and R. M. Lambert, *Surf. Sci.* **282**, 205 (1993).

¹⁰K. Wilson, A. F. Lee, C. Hardacre, and R. M. Lambert, *J. Phys. Chem. B* **102**, 1736 (1998).

¹¹A. B. McLean, I. T. McGovern, C. Stephens, W. G. Wilke, H. Haak, K. Horn, and W. Braun, *Phys. Rev. B* **38**, 6330(R) (1988); Y. S. Luo, Y.-N. Yang, J. H. Weaver, L. T. Florez, and C. J. Palmström, *ibid.* **49**, 1893 (1994).

¹²J. G. Chen, C. A. Menning, and M. B. Zellner, *Surf. Sci. Rep.* **63**, 201 (2008); U. Bardi, *Rep. Prog. Phys.* **57**, 939 (1994).

- ¹³J. Hafner and M. Krajčí, *Phys. Rev. B* **57**, 2849 (1998).
- ¹⁴C. Biswas, R. S. Dhaka, A. K. Shukla, and S. R. Barman, *Surf. Sci.* **601**, 609 (2007).
- ¹⁵A. K. Shukla, C. Biswas, R. S. Dhaka, S. C. Das, P. Krüger, and S. R. Barman, *Phys. Rev. B* **77**, 195103 (2008).
- ¹⁶A. G. Jackson, M. P. Hooker, and T. W. Haas, *J. Appl. Phys.* **38**, 4998 (1967).
- ¹⁷L. Q. Jiang, M. W. Ruckman, and M. Strongin, *Phys. Rev. B* **39**, 1564 (1989).
- ¹⁸R. J. Smith, A. W. D. van der Gon, and J. F. van der Veen, *Phys. Rev. B* **38**, 12712 (1988).
- ¹⁹J. E. Kirsch and C. J. Tainter, *Surf. Sci.* **602**, 943 (2008).
- ²⁰A. K. Shukla, P. Krüger, R. S. Dhaka, D. I. Sayago, K. Horn, and S. R. Barman, *Phys. Rev. B* **75**, 235419 (2007).
- ²¹A. K. Shukla, R. S. Dhaka, S. W. D'Souza, M. Maniraj, S. R. Barman, K. Horn, Ph. Ebert, K. Urban, D. Wu, and T. A. Lograsso, *J. Phys. Condens. Matter* **21**, 405005 (2009).
- ²²K. J. S. Sawhney, F. Senf, M. Scheer, F. Schiifers, J. Bahrtdt, A. Gaupp, and W. Gudat, *Nucl. Instrum. Methods Phys. Res. A* **390**, 395 (1997).
- ²³R. S. Dhaka and S. R. Barman, *Phys. Rev. B* **79**, 125409 (2009); R. S. Dhaka, C. Biswas, A. K. Shukla, S. R. Barman, and A. Chakrabarti, *ibid.* **77**, 104119 (2008).
- ²⁴A. K. Shukla, S. Banik, R. S. Dhaka, C. Biswas, S. R. Barman, and H. Haak, *Rev. Sci. Instrum.* **75**, 4467 (2004).
- ²⁵R. S. Dhaka, A. K. Shukla, M. Maniraj, S. W. D'Souza, J. Nayak, and S. R. Barman, *Rev. Sci. Instrum.* **81**, 043907 (2010).
- ²⁶J. C. Slater, *J. Chem. Phys.* **41**, 3199 (1964).
- ²⁷S. Doniach and M. Sunjić, *J. Phys. C* **3**, 285 (1970).
- ²⁸C. Biswas, A. K. Shukla, S. Banik, S. R. Barman, and A. Chakrabarti, *Phys. Rev. Lett.* **92**, 115506 (2004).
- ²⁹W. Theis and K. Horn, *Phys. Rev. B* **47**, 16060 (1993).
- ³⁰M. P. Seah and W. A. Dench, *Surf. Interface Anal.* **1**, 2 (1979). The equation $\lambda_m(E) = 538E^{-2} + 0.41(aE)^{1/2}$ has been used where $\lambda_m(E)$ is the inelastic mean free path in ML at photoelectron kinetic-energy E in electron volts and a is the thickness of one ML in nanometers.
- ³¹J. D. R. Buchanan, T. P. A. Hase, B. K. Tanner, P. J. Chen, L. Gan, C. J. Powell, and W. F. Egelhoff Jr., *Phys. Rev. B* **66**, 104427 (2002).
- ³²J. J. Yeh and I. Lindau, *At. Data Nucl. Data Tables* **32**, 1 (1985).
- ³³C. Biswas, A. K. Shukla, S. Banik, V. K. Ahire, and S. R. Barman, *Phys. Rev. B* **67**, 165416 (2003); S. R. Barman, P. Häberle, and K. Horn, *ibid.* **58**, R4285 (1998).
- ³⁴R. S. Dhaka and S. R. Barman, *Phys. Rev. Lett.* **104**, 036803 (2010).
- ³⁵A. K. Shukla, R. S. Dhaka, C. Biswas, S. Banik, S. R. Barman, K. Horn, Ph. Ebert, and K. Urban, *Phys. Rev. B* **73**, 054432 (2006).
- ³⁶D. Hobbs, J. Hafner, and D. Spisák, *Phys. Rev. B* **68**, 014407 (2003).
- ³⁷F. R. McFeely, S. P. Kowalczyk, L. Ley, and D. A. Shirley, *Solid State Commun.* **15**, 1051 (1974).
- ³⁸C. Binns and C. Norris, *Surf. Sci.* **116**, 338 (1982).